Biomass and Bioenergy 105 (2017) 392–401

Contents lists available at ScienceDirect

Biomass and Bioenergy

journal homepage: http://www.elsevier.com/locate/biombioe

Research paper

Seasonal variability of evapotranspiration and carbon exchanges over a biomass sorghum field in the Southern U.S. Great Plains

Sumit Sharma [a, 1], Nithya Rajan [a, *], Song Cui [b, 2], Kenneth Casey [c], Srinivasulu Ale [b], Russell Jessup [a], Stephen Maas [d]

[a] Department of Soil and Crop Sciences, Texas A&M University, College Station, TX 77843, USA
[b] Texas A&M AgriLife Research and Extension Center, Vernon, TX 76384, USA
[c] Texas A&M AgriLife Research and Extension Center, Amarillo, TX 79106, USA
[d] Department of Plant and Soil Science, Texas Tech University, Lubbock, TX 79409, USA

ARTICLE INFO

Article history:
Received 30 April 2017
Received in revised form
19 July 2017
Accepted 28 July 2017

Keywords:
Bioenergy
Eddy covariance
Sorghum bicolor
Net ecosystem production
Gross primary production
Ecosystem respiration

ABSTRACT

The eddy covariance method was used to investigate carbon fluxes and evapotranspiration (ET) from a high biomass forage sorghum (*Sorghum bicolor* L.) field in the Southern U.S. Great Plains for three growing seasons (2013–2015). Above normal precipitation and narrow row spacing (50 cm) led to higher biomass production (25 Mg ha^{-1}) and leaf area index (LAI = 7.2) development in 2014. This also resulted in higher carbon uptake or net ecosystem production (NEP) and ET during that year. Early and late season precipitation enhanced ecosystem respiration (R_{eco}) resulting in lower NEP in 2015. Shorter growing season (119 days) also contributed to lower cumulative NEP in 2015. Estimated gross primary production (GPP) in 2014 (1780 g m^{-2}) was 10% higher than the GPP in 2013 (1591 g m^{-2}) and 24% higher than the GPP in 2015 (1353 g m^{-2}). During all growing seasons, the site was a source of carbon (negative NEP) at the beginning and transitioned to a sink (positive NEP) later in the season. Biomass-GPP relationship indicated that approximately 65% of total GPP was allocated to above ground biomass (AGB). Average monthly ecosystem WUE (expressed as gross carbon gain per unit of ET) ranged from 1.7 g mm^{-1} to 4.2 g mm^{-1}. Results from our study indicate that weather conditions, growing season length and crop management are important factors in determining the magnitude of carbon uptake and release, and ET of this cellulosic biofuel feedstock crop in the Southern U.S. Great Plains.

1. Introduction

Fuel ethanol production in the U.S. has increased from 40 billion liters in 2009 to 55.6 hm^3 in 2015 [1]. Approximately 3.2 hm^3 of U.S. fuel ethanol was exported to more than 50 countries in 2015 [1]. Although U.S. is the largest exporter of fuel ethanol in the world, it also imported 0.36 hm^3 of ethanol in 2015. Majority of this imported ethanol came from Brazil. The main reason for the import was that the Renewable Fuel Standards (RFS) and the Low Carbon Fuel Standards of California and other states specify the use of biofuels with low greenhouse gas (GHG) emissions [2]. Based on life cycle analyses, GHG emissions from sugarcane (*Saccharum* spp.) cropping systems in Brazil are considered to have less GHG emissions compared to corn (*Zea mays*) cropping systems in the U.S., thus promoting its import [3]. The RFS statutory requirement for renewable fuel production is 113.6 hm^3 in 2020, of which at least 35% of total renewable fuels must be produced from cellulosic biofuels with low GHG emissions [4].

Cellulosic biofuels are produced from lignocellulosic biomass feedstocks using advanced conversion technological processes [5]. The main cellulosic biomass feedstocks include agricultural residues and dedicated herbaceous and woody energy crops [6,7]. Many cellulosic bioenergy crops are ideal candidates for growing in the Southern Great Plains due to their adaptation to water-limited and semi-arid environmental conditions. A potential bioenergy crop that is gaining popularity in the Southern Great Plains is sorghum (*Sorghum bicolor* L.). Several studies have reported the drought tolerance and high water use efficiency (WUE) characteristics of biomass and forage sorghums in the Southern Great Plains

* Corresponding author.
E-mail address: nrajan@tamu.edu (N. Rajan).
[1] Present Address: Department of Plant and Soil Sciences, Oklahoma State University, Stillwater, OK 74078, USA.
[2] Present Address: School of Agribusiness and Agriscience, Middle Tennessee State University, Murfreesboro, TN 37132, USA.

http://dx.doi.org/10.1016/j.biombioe.2017.07.021
0961-9534/

[8–11]. In addition to agronomic characteristics such as high WUE and high biomass production, physical and chemical properties of the feedstocks also play a major role in determining their suitability for biofuel production [12–14]. The brown midrib (*bmr*) cultivars of forage sorghum have lower lignin content, and hence are ideal for ethanol production as lignin tends to prevent the enzymes from accessing cellulose [12,15,16]. Additionally, forage sorghum is cheaper to produce than corn [17]. Several new *bmr* cultivars of forage sorghum have already been successfully introduced in the Southern Great Plains region.

Changes in land surface properties and management practices due to land use change to cellulosic biofuel crops can significantly influence regional carbon and hydrologic cycles [18,19]. In recent years, eddy covariance systems with fast response instruments have been increasingly used for direct measurements of the exchange of CO_2 and water vapor between the vegetation surface and the atmosphere [20–22]. Using this method, CO_2 flux or net ecosystem production (NEP) is determined as the covariance between vertical wind velocity and CO_2 concentration. During the daytime, NEP measured using the eddy covariance method represents the balance between CO_2 absorbed by plants through photosynthesis (gross primary production, GPP) and CO_2 that is released through a combination of autotrophic and heterotrophic respiration (ecosystem respiration, R_{eco}). At night, NEP measurements represent R_{eco}. Similar to NEP, latent heat flux (LE) is determined as the covariance between vertical wind velocity and water vapor concentration. Latent heat is the energy flux used in evapotranspiration (ET). Scientists have established networks of experimental sites such as Ameriflux with eddy covariance systems for quantifying NEP and ET from key ecosystems in North America [23]. Data from these experimental sites are critical for gaining a proper understanding of regional and global carbon and hydrologic cycles. However, very few studies have been conducted to investigate ET and CO_2 fluxes of cellulosic biofuel crops such as sorghum [24]. In this three-year study (2013–2015), we examined half-hourly, daily, and seasonal ET and carbon flux dynamics of annual high biomass forage sorghum in the Southern U.S. Great Plains. Our results provide further insights into the dynamics of carbon fluxes and ET for this lesser studied, yet crucial, cellulosic biofuel cropping system in the Southern U.S. Great Plains.

2. Materials and methods

2.1. Study site

The study was conducted in a farmer's center-pivot irrigated field planted to high biomass forage sorghum for commercial seed production. The field was located approximately 4.5 km northeast of Plainview, TX in the Southern Great Plains region (34°12′34.70″ N and 101°37′50.85″ W, 1100 m elevation). The climate of the region is semiarid with long-term mean annual rainfall of 460 mm [25]. The total area of the center pivot field was 0.5 km^2 (50 ha) and sorghum was planted to half of the area (0.25 km^2). Remaining half of the field was planted to cotton (*Gossypium hirsutum* L.). The farmer practiced an annual rotation of sorghum and cotton in these two sections. The sorghum cultivar planted was Surpass XL *bmr* (Coffey Seed Company, Plainview, TX). The crop was planted on 20 May (DOY 140) in 2013 and 2014. Heavy rains in 2015 delayed planting, thus the crop was planted on June 4 (DOY 155) that year. In all three years, the planting density was approximately 120,000 plants per hectare. However, the row spacing was narrower in 2014 (50 cm) compared to 2013 and 2015 (100 cm). Urea (46-0-0) was broadcasted in the field in spring before planting at a rate of 325 kg ha^{-1}. In addition, triple superphosphate (0-45-0) was applied at a rate of 65 kg ha^{-1} prior to planting. For the first 40 days, the field was supplied with approximately 19 mm of water during each irrigation event. For the rest of the season, the field was irrigated with 38 mm of water during each irrigation event. Overall, the field was supplied with 400 mm of irrigation water in 2013 (12 irrigations) and 2014 (13 irrigations), and 267 mm of irrigation water in 2015 (7 irrigations). The field was harvested at physiological maturity for seed on 8 October in 2013 (DOY 282), 11 October in 2014 (DOY 285), and 1 October in 2015 (DOY 275). The growing season was 140, 147, and 119 days long in 2013, 2014, and 2015, respectively. Since the farmer practiced crop rotation, the field was disked in early spring to incorporate residues. The field was disked again before planting and was cultivated twice in June to control weeds. The major soil at the study site is Pullman Clay Loam (a fine, mixed, superactive, thermic Torrertic Paleustoll) with 0–1% slope.

2.2. Eddy covariance and ancillary data collection

Continuous measurements of CO_2 and water vapor were made using an eddy covariance flux tower established in the field at planting. Wind speed, CO_2, and water vapor concentrations were measured using IRGASON, which is an integrated open-path infrared gas analyzer (IRGA, Model EC-150, Campbell Scientific Inc., Logan, UT, USA) and sonic anemometer (Model CSAT-3A, Campbell Scientific Inc., Logan, UT, USA) system. These instruments were set up facing southwest (into the prevailing wind direction) at 2 m above the ground level at the beginning of the season. The instruments were raised to 2.6 m above the ground level as the average plant height increased to a maximum of 1.3 m. The movement of the irrigation system did not interfere with data collection as the height of the center-pivot system was over 3 m. The fetch (distance from boundary of the field to the tower) was about 200 m in east and west directions, and about 350 m in north and south directions. Data from the CSAT3A sonic anemometer and EC150 system were measured at 10-Hz sampling rate using a CR3000 datalogger (Campbell Scientific Inc., Logan, UT, USA). The raw 10-Hz wind velocity, CO_2, and water vapor data from CSAT3A sonic anemometer and EC150 were saved for further post-processing and analysis of NEP, GPP, R_{eco} and ET.

Other environmental variables measured include air temperature (T_{air}) and relative humidity (RH) (HMP50, Campbell Scientific Inc., Logan, UT, USA), net radiation (R_n) (NR-Lite net radiometer, Kipp & Zonen, Delft, The Netherlands), photosynthetically active radiation (PAR) (LI-200SL quantum sensor, LI-COR Biosciences, Lincoln, NE, USA), solar irradiance (LI-190SB pyranometer, LI-COR Biosciences, Lincoln, NE, USA), and precipitation (TE525 rain gauge, Campbell Scientific Inc., Logan, UT, USA). Soil temperature (T_{soil}) was measured using two averaging soil thermocouples installed at 2 and 6 cm below the surface (TCAV averaging soil thermocouples, Campbell Scientific Inc., Logan, UT, USA). Soil volumetric water content (VWC) at 4 cm below the surface was measured using two CS616 time domain reflectometer soil moisture sensors (Campbell Scientific Inc., Logan, UT, USA). Soil heat flux at 8 cm below the soil surface (G_{8cm}) was measured using four self-calibrating soil heat flux plates (HFP01SC, Hukseflux, Deft, The Netherlands). All the environmental variables were measured at 5 s interval. The CR3000 datalogger was programmed to calculate and save 30-min average values of these environmental variables.

Soil heat flux at the surface (G) was estimated every 30-min by adding soil heat storage above the heat flux plate (S) to the measured soil heat flux at 8 cm using Eq. [1].

$$G = G_{8cm} + S \quad (1)$$

Heat storage above the heat flux plates was calculated as follows:

$$S = \frac{\Delta T_s C_s d}{t} \quad (2)$$

where S is heat storage, ΔT_s is the temporal change in T_{soil} (difference between two consecutive 30 min observations), d is depth of soil in meters above soil heat flux plate, C_s is the heat capacity of moist soil, and t is time in seconds. Heat capacity of soil in Eq. (1) can be calculated using bulk density ($\rho_b = 1.3$ g cm^{-3}), volumetric water content (θ_v) at 4 cm depth, density of water ($\rho_w = 1000$ kg m^{-3}), heat capacity of water ($C_w = 4.2$ kJ kg^{-1}K^{-1}), and heat capacity of dry mineral soil ($C_d = 840$ J kg^{-1} K^{-1}) as follows:

$$C_s = \rho_b C_d + \theta_v \rho_w C_w \quad (3)$$

Measurements of phenological development were started once the plant stand was well established (June). Data were collected at weekly intervals in 2013 and at bi-weekly intervals in 2014 and 2015 growing seasons. Plant measurements collected include leaf area index (LAI) and above ground biomass (AGB). Plant samples were taken randomly from the field to measure LAI and AGB. Plants were stored in an ice chest in the field and leaf area was measured (after separating leaves from shoots) using a leaf area meter (Model LI-3100, Licor Biosciences, Lincoln, NE, USA) immediately after they were brought to the laboratory. Plant density (number of plants per m^2) and leaf area were used to calculate the LAI.

2.3. Eddy covariance data processing and analysis

Using the eddy covariance method, half-hourly fluxes of CO_2 and LE were calculated as the covariance between fluctuations from the mean vertical wind speed and corresponding fluctuations of CO_2 and water vapor. The sensible heat flux (H) was calculated similarly using vertical wind speed and T_{air}. The open source EddyPro 4.0 software (LI-COR Biosciences, Lincoln, NE, USA) was used to compute half-hourly fluxes. Calculation of fluxes requires a series of operations including raw data filtering and applications of algorithms for calculating and correcting fluxes. Some of these corrections include spike removal, spectral corrections for flux losses [26], and corrections for air density fluctuations [27]. EddyPro assigns quality flags based on widely used tests for steady state and turbulence [28,29]. The flag '0' indicates high quality fluxes and '1' indicates intermediate quality fluxes. All poor quality fluxes are flagged as '2'. The processed half-hourly fluxes were subjected to additional quality control before gap filling. In addition to 30 min data that were flagged as '2', data were screened and filtered for physically implausible values occurred during precipitation, equipment maintenance, and low turbulence conditions (when the friction velocity was <0.10 m s^{-1}).

All missing and poor quality 30 min flux data (NEP, LE and H) were gapfilled using the on-line CarboEurope and Fluxnet eddy covariance gap-filling tool [30]. This online tool uses methods similar to those described in Falge et al. [31] and Reichstein et al. [32]. Small gaps in the data (4 half-hour periods or less) were filled by linear interpolation. Larger gaps were filled by the average values calculated using look up tables within a certain time window under similar meteorological conditions. Similarity between meteorological conditions was determined when deviation in solar irradiance was not more than 50 W m^{-2}, T_{air} was not more than 2.5 °C and vapor pressure deficit (VPD) was within 0.5 kPa. The standard time window was ±7 days, which was expanded to ±14 days in case similarity in meteorological conditions were not present within the 7 days window. This online tool also partitioned NEP and provided estimations of half-hourly GPP and R_{eco} using an established flux-partitioning approach [31,32]. Night-time (solar irradiance less than 20 W m^{-2}) NEP values represent R_{eco}. Following Lloyd and Taylor [33], short-term temperature sensitivity equations developed between original night-time NEP measurements (quality flag '0') and corresponding soil temperature (T_{soil}) measurements made at the 4-cm depth. Half-hourly daytime R_{eco} was modeled using these temperature sensitivity relationships. Half-hourly GPP was estimated as the difference between R_{eco} and NEP. Additional details on gap-filling and flux partitioning procedure can be found in Falge et al. [31] and Reichstein et al. [32].

2.4. Energy balance

We examined the main components of energy balance which include LE, H, R_n and G. For this study, the steady state surface energy balance was defined by the equation,

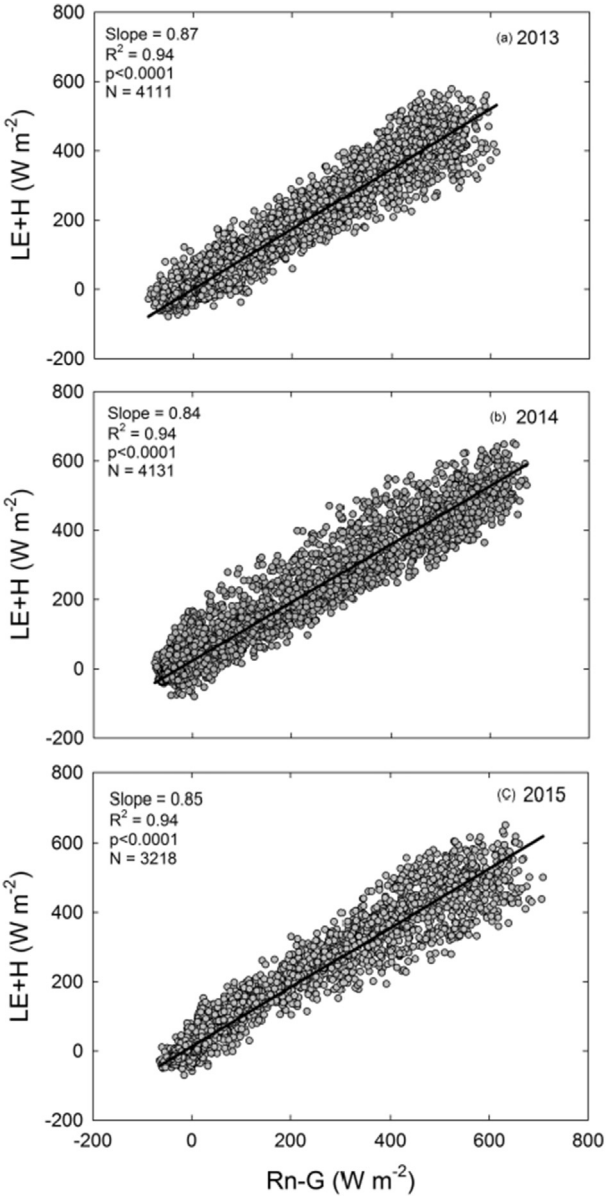

Fig. 1. The 30-min averages of the balance of net radiation (R_n) and soil heat (G) fluxes plotted versus corresponding values of the sum of latent heat (LE) and sensible heat (H) fluxes for (a) 2013, (b) 2014, and (c) 2015. The solid line represents the regression through the points.

$$R_n - G = LE + H \quad (4)$$

where R_n is net radiation flux density (W m^{-2}), G is the soil heat flux density (W m^{-2}), LE is the latent heat flux density (W m^{-2}) and H is the sensible heat flux density (W m^{-2}). The difference between R_n and G represents the available energy at the surface. We assumed negligible net horizontal advection of energy and heat storage within the canopy. Surface energy balance was examined by plotting thirty-minute averages of R_n - G vs. corresponding values of the sum of LE and H. The slope of the regression through the distribution of points is an indication of the degree of closure of the steady-state energy balance with a slope of 1 indicating complete closure and a slope <1 indicating partial closure.

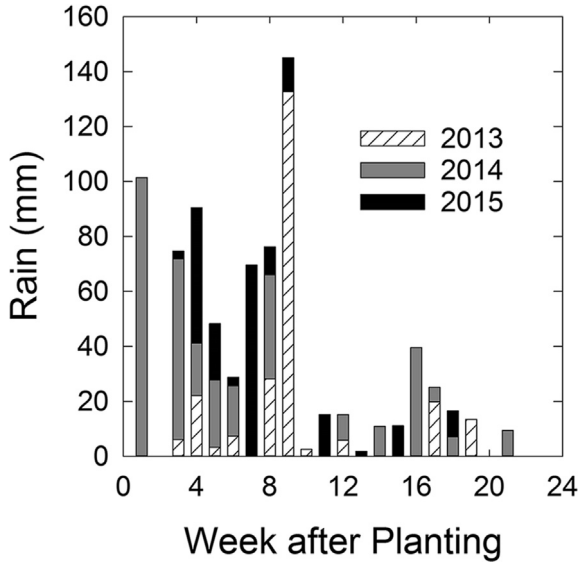

Fig. 2. Weekly averages of precipitation in mm for the 2013 (DOY 140-282), 2014 (DOY 140-285), and 2015 (DOY 155-275) growing seasons. Error bars represent standard error of the mean.

2.5. Water use efficiency

Ecosystem WUE at daily, monthly, and seasonal scales were calculated by dividing daytime cumulative GPP by daytime cumulative ET at daily, monthly, and seasonal time scales, respectively as shown in Eq. (5).

$$\mathrm{WUE} = \frac{\mathrm{GPP}}{\mathrm{ET}} \quad (5)$$

3. Results & discussion

3.1. Energy balance

Seasonal energy balance was calculated using half-hourly turbulent fluxes (LE and H) and available energy (R_n and G) components. Data were included in the analysis only when all four measurements were available. The sum of half-hourly LE and H was strongly correlated to the sum of available energy (R_n-G) in all three years with an R^2 value of 0.94 (Fig. 1). The slopes of the regression

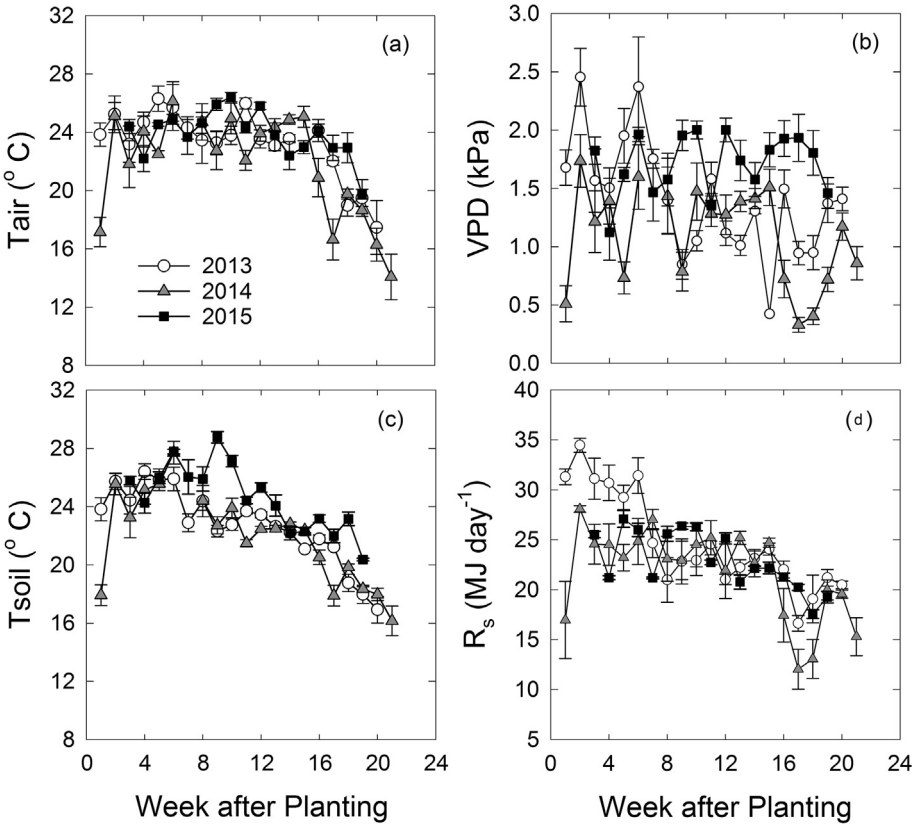

Fig. 3. Weekly averages of meteorological variables for the 2013 (DOY 140-282), 2014 (DOY 140-285), and 2015 (DOY 155-275) growing seasons: (a) air temperature (T_{air}) in °C, (b) vapor pressure deficit (VPD) in kPa, (c) soil temperature (T_{soil}) at 4 cm depth in °C, and (d) solar irradiance (R_s) in MJ day^{-1}. Error bars represent standard error of the mean.

lines were 0.87, 0.84 and 0.85 for 2013, 2014, and 2015, respectively, indicating that 84–87% of the variation in available energy (R_n-G) was accounted for by the sum of the turbulent energy fluxes (Fig. 1). This degree of energy balance closure at our site is similar to those reported in other studies. Foken [34] reported that energy balance was in the range of 70–90% for a variety of ecosystems studied using eddy covariance measurements. Wagle and Kakani [24] reported closure on the order of 77% for a biomass sorghum field in the Southern Great Plains. Rajan et al. [20,35] reported energy balance in the range of 80–90% for cotton and improved pasture fields in the Southern Great Plains. In our study, we did not consider residual energy terms associated with radiant energy used in photosynthesis and heat energy transiently stored in the canopy.

3.2. Meteorological conditions and plant phenology

Weekly average environmental data from the site is presented in Figs. 2 and 3. The 2013 growing season precipitation (235 mm) was less than the precipitation received in 2014 (328 mm) and 2015 (271 mm). The distribution of precipitation over the growing season also varied among the three study years (Fig. 2). This resulted in differences in weekly average VPD and solar irradiance among the three study years (Fig. 3). Weekly average VPD over the course of the growing season ranged from 0.42 to 2.4 kPa in 2013, 0.33–1.7 kPa in 2014 and 1.1–1.9 kPa in 2015. Weekly averages of air and soil temperatures were closely correlated (R = 0.91 in 2013 and 2014 and R = 0.84 in 2015). Early in the season (May and June), average T_{soil} was slightly higher than T_{air} which decreased to below T_{air} later in the season. Weekly average T_{air} during study period ranged from 17.5 to 26.3 °C in 2013, 14.1–26.1 °C in 2014, and 19.8–26.4 °C in 2015. Average T_{air} for the growing season was 23.2 °C in 2013, 21.9 °C in 2014, and 23.9 °C in 2015. In 2013 and 2015, seasonal average T_{air} was close to the thirty year (1981–2010) average temperature of 23.6 °C (U.S. Climate Data available at: http://www.usclimatedata.com/) for the corresponding period. In 2014, seasonal average T_{air} was approximately 2 °C less than the long-term average temperature. The average daily T_{air} during the first week after planting in 2014 was approximately 8 °C less than the T_{air} during the corresponding period in 2013 (Fig. 3a). Similar to T_{air}, the average daily T_{soil} during the first week after planting in 2014 was approximately 6 °C lower than the T_{soil} during the corresponding period in 2013. Year 2014 also had low growing season average T_{soil} (21.9 °C) compared to 2013 (22.8 °C) and 2015 (24.6 °C). Spring 2014 was cooler than normal and the low air and soil temperatures were due to many late spring cold fronts passing over the region.

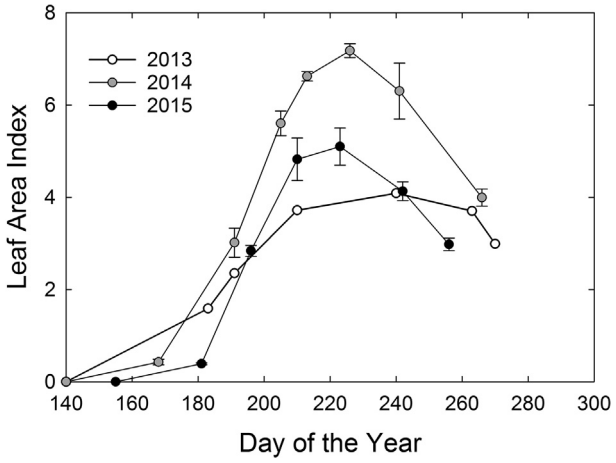

Fig. 4. Seasonal evolution of leaf area index (LAI) of sorghum in 2013, 2014 and 2015. Error bars represent standard error of the mean. No replications were conducted in the 2013 growing season.

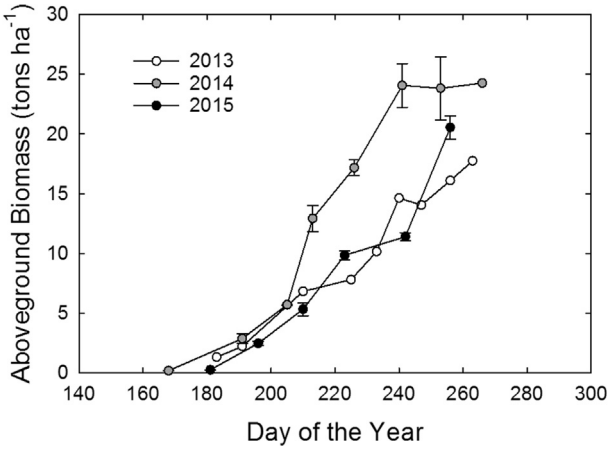

Fig. 5. Seasonal evolution of above ground biomass (AGB) of sorghum in 2013, 2014 and 2015. Error bars represent standard error of the mean. No replications were conducted in the 2013 growing season.

In all three years, LAI changed rapidly during the growing season. The maximum LAI measured was 4.1 in 2013, 7.2 in 2014 and 5.1 in 2015 (Fig. 4). In 2015, the maximum LAI was observed approximately 2- weeks later than in 2013 and 2014 due to delayed planting. In all three years, LAI remained at its peak for approximately 2 weeks. Aboveground biomass increased significantly from

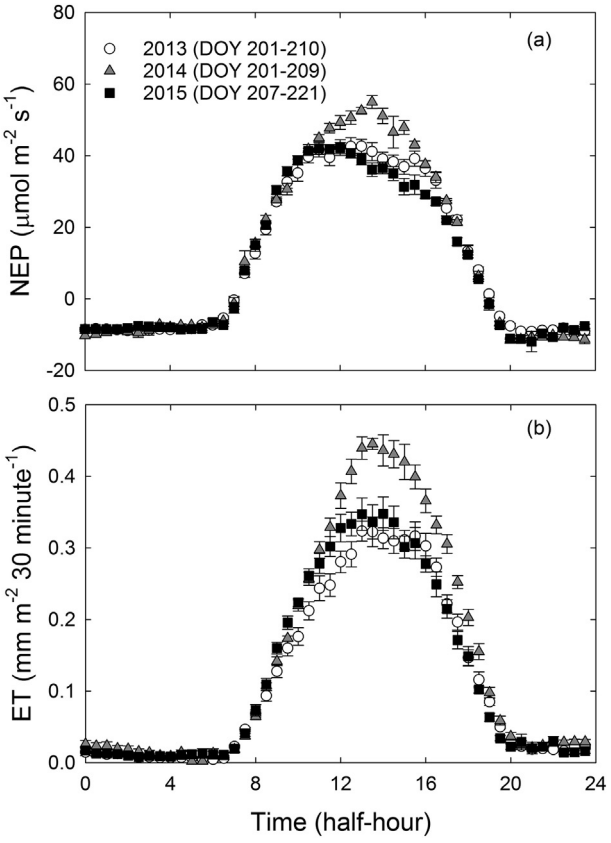

Fig. 6. Diurnal patterns of half-hourly net ecosystem production (NEP) and evapotranspiration (ET) during the flag leaf period in 2013 (DOY 201-210), 2014 (DOY 201-209) and 2015 (DOY 214-221). Only measured data during clear sky conditions were used. Error bars represent standard error of the mean.

June to September. Peak AGB measured was 18 Mg ha^{-1} in 2013, 25 Mg ha^{-1} in 2014, and 21 Mg ha^{-1} in 2015 (Fig. 5). The inter-annual variation in LAI and AGB was primarily due to the difference in plant population density. Plant density was higher in 2014 (11 m^{-2}) compared to that in 2013 (8.33 m^{-2}) and 2015 (9.25 m^{-2}). The higher plant density in 2014 was due to narrower row spacing. The influence of plant density on LAI and biomass has been reported in several previous studies [36–38].

The growth period of sorghum from emergence to maturity was approximately 100 days in our study. Even without a second harvest, the biomass production of sorghum at our study site was comparable to the seasonal biomass production of several other bioenergy crops in the U.S [39]. Researchers have reported the yield of biomass sorghum ranging from less than 10 Mg ha^{-1} to over 30 Mg ha^{-1}, depending on the region and growing conditions. Oikawa et al. [40] reported dry biomass production of sorghum ranging from 11.7 Mg ha^{-1} to 16.2 Mg ha^{-1} for three harvests between February and November in California. In Florida, Singh et al. [41] reported AGB production of 19.4 Mg ha^{-1} for biomass sorghum. Cotton et al. [42] reported dry biomass yield for forage sorghum ranging from 13.2 to 30.1 Mg ha^{-1} in the Texas High Plains. These authors reported that the biomass yield varied depending upon irrigation level and cultivar characteristics. Results from our study suggest that high biomass forage sorghum could be a promising biomass crop in the semi-arid Southern Great Plains under irrigated conditions. Additionally, several researches have reported ratooning capabilities of sorghum in the Southern U.S. [43]. Ratoon crop yields are highly variable depending on factors such as environmental conditions (for example, water stress), pest issues, crop growth stage at first harvest, genetic makeup and physiology of cultivars [44,45]. McCormick et al. [43] demonstrated ratooning capabilities of sorghum without compromising the yield from multiple harvests in Franklinton, LA. The short growing period of sorghum to reach maturity in the Southern U.S. Great Plains also suggests double-cropping possibilities with winter wheat or other short duration crops in the region.

3.3. Diurnal variations: Net ecosystem production and evapotranspiration

We compared diurnal changes in NEP and ET at the peak crop growth stage (flag leaf) in all three years by plotting half-hourly values (Fig. 6). The diurnal half-hourly averages of meteorological variables (PAR, R_n, T_{air}, and VPD) during the same measurement period are presented in Fig. 7. The maximum T_{air} was 33.1 °C in 2014 and 33.6 °C in 2015 (Fig. 7d). In 2013, T_{air} during the same time period was 4 °C lower with a maximum of 29.6 °C. Although T_{air} was similar in 2014 and 2015, the VPD was higher in 2015 compared to 2014 (Fig. 7c). Daytime VPD was the lowest in 2013 (Fig. 7c). The maximum half-hourly measured NEP was 55.0 μmol m^{-2} s^{-1} in 2014, whereas the peak half-hourly NEP was approximately 42.6 μmol m^{-2} s^{-1} in 2013 and 42.8 μmol m^{-2} s^{-1} in 2015 (Fig. 6a). Similar to NEP, ET was high in 2014 compared to 2013 and 2015 (Fig. 6b). The maximum half-hourly measured ET was 0.45 mm in 2014, 0.32 mm in 2013 and 0.35 mm in 2015. Average daily ET during the peak growth stage was 5.55 mm day^{-1} in 2013, 7.06 mm day^{-1} in 2014 and 5.91 mm day^{-1} in 2015. Low VPD and air temperature combined with lower LAI during the peak growth stage in 2013 resulted in the lowest measured ET among the three study seasons. The amount of leaf area exerts a major influence in mediating diurnal changes in carbon exchange and ET from ecosystems [46,47]. Due to narrower row spacing and higher plant density, LAI in 2014 was approximately 75% higher compared to leaf area in 2013 and 40% higher compared to leaf area in 2015. The high

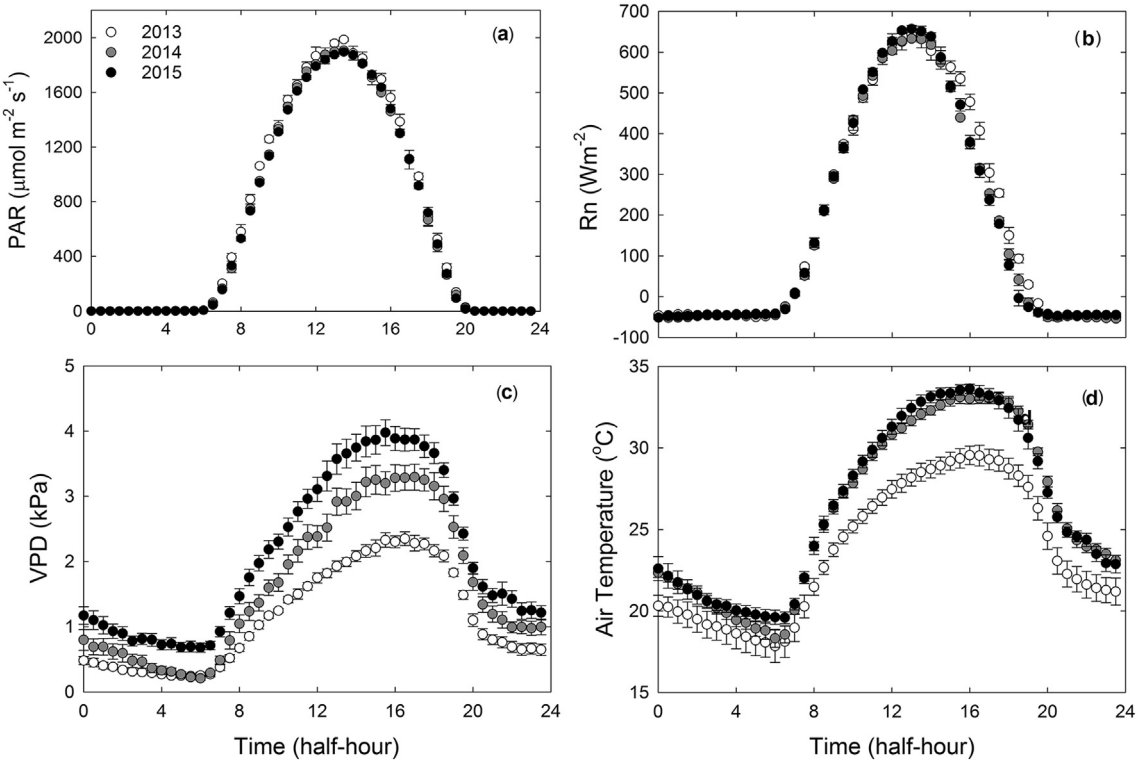

Fig. 7. Diurnal patterns of half-hourly measurements of (a) photosynthetically active radiation (PAR) (b) net radiation (R_n), (c) vapor pressure deficit (VPD), and (d) air temperature (T_{air}) during the flag leaf period in 2013 (DOY 201-210), 2014 (DOY 201-209) and 2015 (DOY 214-221). Only measured data during clear sky conditions were used. Error bars represent standard error of the mean.

LAI and canopy closure in 2014 effectively increased evaporative surface area and light-harvesting efficiency resulting in higher CO_2 uptake and ET that year. Increases in ET and NEP with increasing leaf area has been reported for both managed and natural ecosystems [48,49]. In 2014, CO_2 uptake (NEP) increased as PAR increased and peaked around solar noon time (13:00) when PAR was the highest. However, in 2013 and 2014, carbon uptake peaked 2 h earlier (11:00) and remained relatively constant until 13:00, and declined thereafter. Many scientists have reported saturation of NEP at high levels of PAR [50,51]. The average nighttime loss of CO_2 to the atmosphere was slightly higher in 2014 (10.4 μmol m^{-2} s^{-1}) compared to other years (8.6 μmol m^{-2} s^{-1} in 2013 and 2015). The maximum value of NEP and ET for this sorghum field was higher than that of a non-irrigated biomass sorghum field in Oklahoma [10,52]. Similar maximum NEP values (68 μmol m^{-2} s^{-1}) were reported by Oikawa et al. [40] for an irrigated biomass sorghum field in California.

3.4. Seasonal variations in carbon exchange

Daily and seasonal cumulative estimates of NEP, GPP and R_{eco} are presented in Fig. 8a–f. During all growing seasons, the site was a source of carbon (negative NEP) at the beginning and transitioned to a sink (positive NEP) later in the season. Carbon uptake peaked in July and August. The maximum daily NEP (net carbon gain) was 13.3 g m^{-2} in 2013 (DOY 199), 14.5 g m^{-2} in 2014 (DOY 202) and 12.3 g m^{-2} in 2015 (DOY 216). Cumulative net carbon uptake during growing season was 710.3 g m^{-2} in 2013, 665.3 g m^{-2} in 2014, and 471.0 g m^{-2} in 2015. Similar to NEP, GPP peaked in July and August across all growing seasons. Maximum daily GPP (gross carbon uptake) estimated was 22.8 g m^{-2} (DOY 203) in 2013 and 26.4 g m^{-2} (DOY 204) in 2014, and 21.9 g m^{-2} (DOY 216) in 2015. Shorter growing season contributed to lower cumulative GPP in 2015. Cumulative seasonal GPP of sorghum was 1591 g m^{-2} in 2013, 1780 g m^{-2} in 2014, and 1353 g m^{-2} in 2015. In all three years, days with the highest respiration occurred after precipitation or

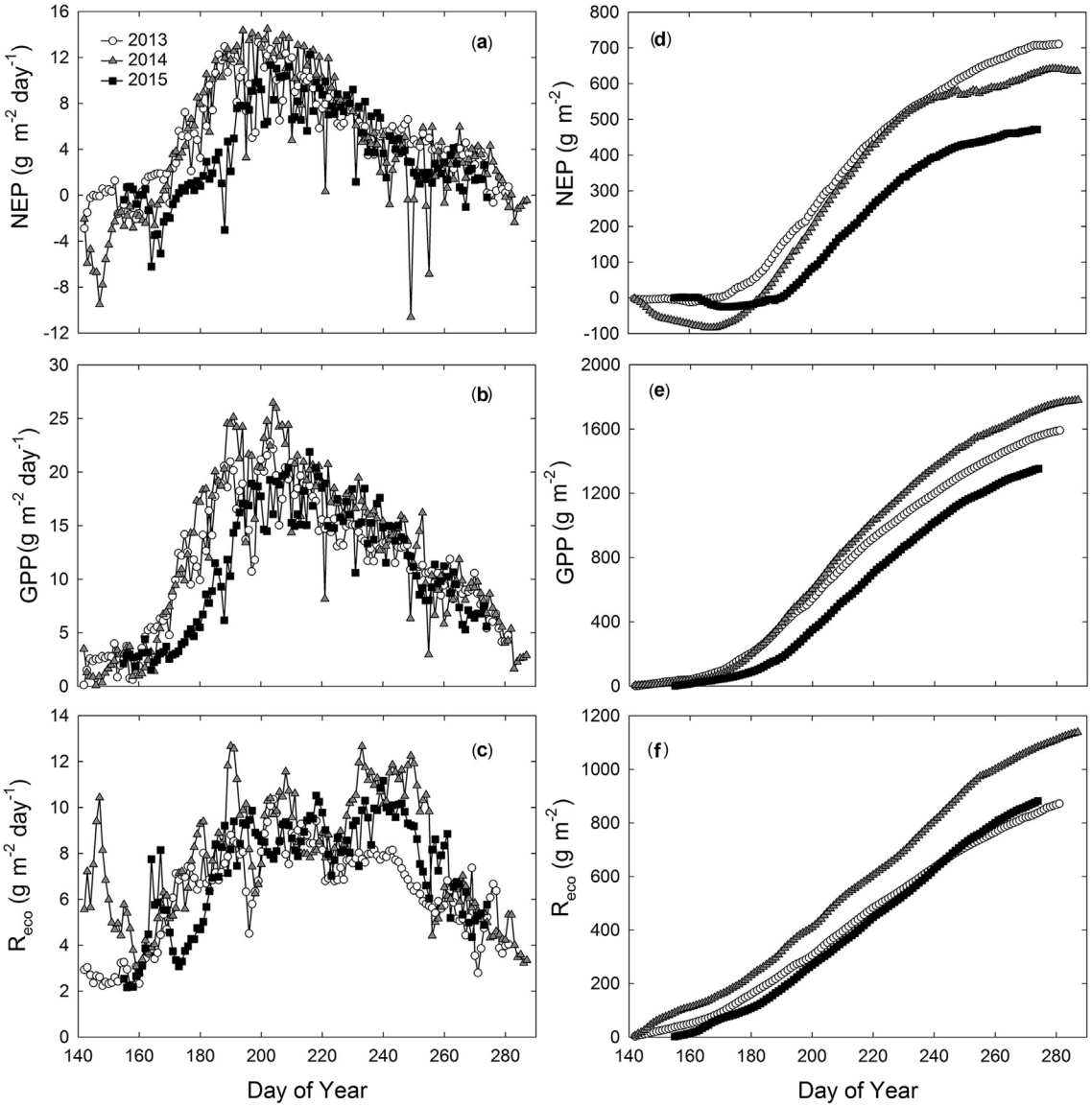

Fig. 8. Carbon exchange variables during the growing season for the high biomass forage sorghum field in the Southern U.S. Great Plains. (a) Daily net ecosystem production (NEP) in 2013, 2014 and 2015, (b) gross primary production (GPP) in 2013, 2014 and 2015 and (c) ecosystem respiration (R_{eco}) in 2013, 2014 and 2015. Cumulative fluxes of carbon exchange variables during the growing season: (d) NEP, (e) GPP, and (f) R_{eco}.

irrigation. Total R_{eco} includes components of autotrophic respiration and heterotrophic respiration by plant roots, microorganisms and soil fauna. The intermittent peaks in R_{eco} (Fig. 8c) were respiration pulses associated with enhanced microbial activity due to precipitation or irrigation. The relative magnitude of R_{eco} in comparison to GPP was greater in 2014 and 2015 than 2013. Ecosystem respiration was 55% of GPP in 2013, and about 65% of GPP in 2014 and 2015. Years 2014 and 2015 registered greater R_{eco} at early and late growing seasons following precipitation events. Cumulative R_{eco} (carbon loss) was 872.1 g m^{-2}, 1138.4 g m^{-2}, and 882.2 g m^{-2} in 2013, 2014 and 2015, respectively. It should be noted that NEP was greater in 2013 despite lower GPP due to proportionately lower R_{eco} during that year compared to 2014 and 2015. Longer growing season and greater LAI contributed towards higher GPP in 2014 than 2013 and 2015. Canopy development is an important determinant of light interception, hence influences GPP and carbon balance [46,47,53–56].

We calculated carbon amount in the AGB assuming 50% carbon in biomass [57]. The carbon content of AGB was a strong linear function of the cumulative GPP. Gross primary production is mainly distributed among AGB, below ground biomass and autotrophic respiration [58]. Combined above and below ground biomass components constitute net primary production. The slope of AGB and GPP relationship was about 0.65, which indicates that 65% of total GPP was allocated to AGB (Fig. 9). Remaining GPP is part of below ground biomass and autotrophic respiration. Campioli et al. [58] obtained a similar relationship for managed and unmanaged ecosystems, including forests, grasslands, and croplands. The authors concluded that managed systems favor allocation of more carbon to AGB due to better nutrient influxes from soil. However, our estimates of carbon allocation to AGB are greater (65%) than those reported by Campioli et al. [58] for managed croplands (about 50%). Allocation of biomass to different parts is an adaptation strategy for different types of vegetation [59]. For example, Blum and Arkin [60] reported that sorghum plants growing under water stressed conditions had deep and uniform roots while well irrigated sorghum plants had a high concentration of roots in shallower soil. This suggests that good management in terms of nutrients and water at our study site might have been responsible for higher carbon allocation to AGB.

3.5. Water use efficiency and evapotranspiration

Table 1 shows cumulative GPP, cumulative ET and WUE calculated for different time periods. Cumulative ET was the highest in 2014 (522 mm), followed by 2013 (495 mm) and 2015 (423 mm). The higher ET in 2014 was in part due to higher water input that year (728 mm through irrigation and precipitation). Measured ET was 72% of total water input in 2014. As discussed previously, higher LAI was another major factor that influenced ET that year. The total water input through irrigation and precipitation was 635 mm in 2013, of which 78% was lost as ET. In 2015, ET was 78% of total water input (538 mm). During all three years, cumulative ET and GPP for July and August were higher than for other months. There was a strong agreement between monthly ET and monthly GPP (Fig. 10). Monthly WUE was calculated as the ratio of monthly cumulative GPP to monthly cumulative ET. Monthly WUE (expressed as gross carbon gain per unit of ET) for the three years was the lowest in June, ranging from 1.7 g mm^{-1} in 2015 to 2.3 g mm^{-1} in 2014. In other months, WUE ranged from 3.0 g mm^{-1} to 4.2 g mm^{-1}. On average, monthly WUE was the highest in 2014 (3.5 g mm^{-1}) and lowest in 2015 (3.0 g mm^{-1}). Higher WUE in 2014 might have been due to reduced loss of water through soil evaporation due to narrower row spacing [61]. The slope of the linear relationship between GPP and ET represents overall WUE, which was 4.5 g mm^{-1} water in our study. The ecosystem WUE estimated in our study was higher than that reported by Wagle et al. [24] for forage sorghum under rainfed conditions in Oklahoma. The authors reported seasonal WUE of 2.47 g mm^{-1} water. For other bioenergy crops, Eichelmann et al. [62] reported WUE of 3.7 g mm^{-1} water for rainfed switchgrass in Canada and Wagle et al. [24] reported 3.2 g mm^{1} water for rainfed switchgrass in Oklahoma. The higher WUE of sorghum in our study is comparable to that of corn (4.1 g mm^{-1} water) reported by Abraha et al. [63] for the U.S. Midwest. Unlike less intensively managed switchgrass fields, our sorghum field was intensively managed with fertilizer application and irrigation to boost production. Thus, the relatively high WUE of forage sorghum at our site is not surprising.

Table 1
Cumulative gross primary production (GPP), evapotranspiration (ET), and ecosystem water use efficiency (WUE) in 2013, 2014, and 2015 growing seasons. WUE is expressed as gross carbon gain (g m^{-2}) per unit of ET (mm).

Year	GPP (g m^{-2})	ET (mm)	WUE (g mm^{-1})
2013	1591	495	3.2
2014	1780	522	3.4
2015	1353	423	3.2

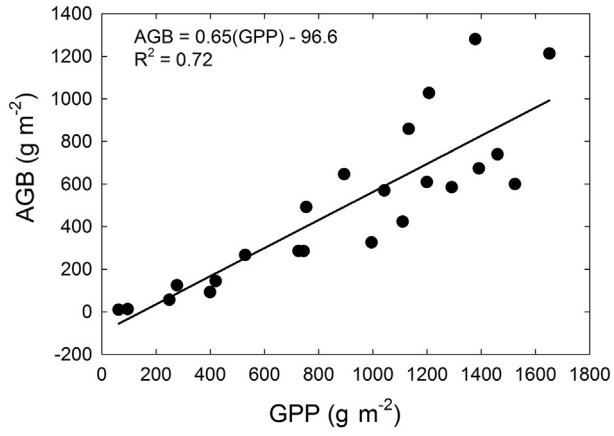

Fig. 9. Cumulative gross primary production (GPP) plotted versus above ground biomass (AGB) carbon.

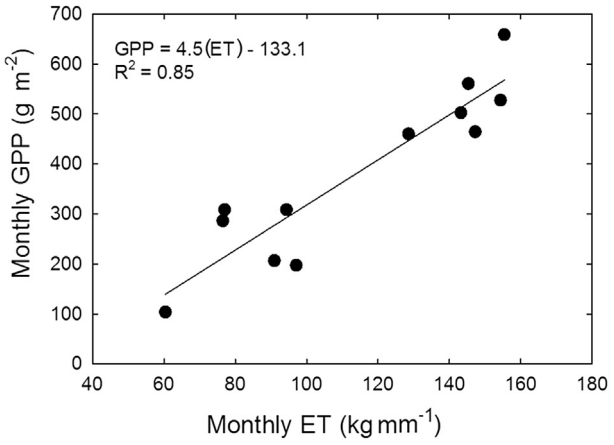

Fig. 10. Relationship between monthly integrals of gross primary production (GPP) and evapotranspiration (ET) during the active growing season (June–September) across all three years (2013–2015). Coefficient of determination (R^2) was 0.89.

4. Conclusions

Eddy covariance measurements made on a high biomass forage sorghum field in the semi-arid Southern Great Plains demonstrated that the dynamics of carbon fluxes and ET were strongly affected by weather conditions, growing season length and crop management (row spacing and irrigation). The year-to-year variability in ET and carbon uptake was mainly explained by variations in leaf area development. Irrigated sorghum in this study was found to be more water use efficient compared to similar cropping systems under rainfed conditions in the Southern Great Plains. As the demand for cellulosic biofuels is increasing, observations from field experiments quantifying seasonal changes in carbon, ET and energy balance could be important in understanding the contributions of large-scale production of cellulosic biofuel feedstock crops to regional weather, carbon and hydrologic cycles.

Acknowledgement

This material is based upon work that is supported by the National Institute of Food and Agriculture, U.S. Department of Agriculture, under award number NIFA-2012-67009-19595. Any opinions, findings, conclusions or recommendations expressed in this publication are those of the author(s) and do not necessarily reflect the view of the U.S. Department of Agriculture.

References

[1] Fueling a High Octane Future, 2016 Ethanol Industry Outlook. Renewable Fuels Association, 2016, p. 40.
[2] J. Whistance, W. Thompson, S. Meyer, Interactions between California's low carbon fuel standard and the national renewable fuel standard, Energy Policy 101 (2017) 447–455, http://dx.doi.org/10.1016/j.enpol.2016.10.040.
[3] C.L. Crago, M. Khanna, J. Barton, E. Giuliani, W. Amaral, Competitiveness of Brazilian sugarcane ethanol compared to US corn ethanol, Energy Policy 38 (11) (2010) 7404–7415.
[4] EPA, Overview for renewable fuel standard. https://www.epa.gov/renewable-fuel-standard-program/overview-renewable-fuel-standard, 2017. (Accessed 15 January 2017).
[5] S.N. Naik, V.V. Goud, P.K. Rout, A.K. Dalai, Production of first and second generation biofuels: a comprehensive review, Renew. Sustain. Energy Rev. 14 (2010) 578–597, http://dx.doi.org/10.1016/j.rser.2009.10.003.
[6] M.A. Sanderson, P.R. Adler, A.A. Boateng, M.D. Casler, G. Sarath, Switchgrass as a biofuels feedstock in the USA, Can. J. Plant Sci. 86 (2006) 1315–1325, http://dx.doi.org/10.4141/P06-136.
[7] P.G. Jefferson, W.P. McCaughey, Switchgrass (Panicum virgatum L.) Cultivar adaptation, biomass production, and cellulose concentration as affected by latitude of origin, ISRN Agron. 2012 (2012) 1–9, http://dx.doi.org/10.5402/2012/763046.
[8] Y. Chen, S. Ale, N. Rajan, C.L.S. Morgan, J. Park, Hydrological responses of land use change from cotton (Gossypium hirsutum L.) to cellulosic bioenergy crops in the Southern High Plains of Texas, USA, GCB Bioenergy 8 (2016) 981–999, http://dx.doi.org/10.1111/gcbb.12304.
[9] B. Hao, Q. Xue, B.W. Bean, W.L. Rooney, J.D. Becker, Biomass production, water and nitrogen use efficiency in photoperiod-sensitive sorghum in the Texas High Plains, Biomass Bioenergy 62 (2014) 108–116, http://dx.doi.org/10.1016/j.biombioe.2014.01.008.
[10] P. Wagle, V.G. Kakani, R.L. Huhnke, Net ecosystem carbon dioxide exchange of dedicated bioenergy feedstocks: switchgrass and high biomass sorghum, Agric. For. Meteorol 207 (2015) 107–116, http://dx.doi.org/10.1016/j.agrformet.2015.03.015.
[11] Y.T. Yimam, T.E. Ochsner, V.G. Kakani, Evapotranspiration partitioning and water use efficiency of switchgrass and biomass sorghum managed for biofuel, Agric. Water Manag. 155 (2015) 40–47, http://dx.doi.org/10.1016/j.agwat.2015.03.018.
[12] D.Y. Corredor, J.M. Salazar, K.L. Hohn, S. Bean, B. Bean, D. Wang, Evaluation and characterization of forage sorghum as feedstock for fermentable sugar production, Appl. Biochem. Biotechnol. 158 (2009) 164–179, http://dx.doi.org/10.1007/s12010-008-8340-y.
[13] A. Karmakar, S. Karmakar, S. Mukherjee, Properties of various plants and animals feedstocks for biodiesel production, Bioresour. Technol. 101 (2010) 7201–7210, http://dx.doi.org/10.1016/j.biortech.2010.04.079.
[14] A.E. Atabani, T.M.I. Mahlia, I. Anjum Badruddin, H.H. Masjuki, W.T. Chong, K.T. Lee, Investigation of physical and chemical properties of potential edible and non-edible feedstocks for biodiesel production, a comparative analysis, Renew. Sustain. Energy Rev. 21 (2013) 749–755, http://dx.doi.org/10.1016/j.rser.2013.01.027.
[15] B.S. Dien, G. Sarath, J.F. Pedersen, S.E. Sattler, H. Chen, D.L. Funnell-Harris, N.N. Nichols, M.A. Cotta, Improved sugar conversion and ethanol yield for forage sorghum (sorghum bicolor L. Moench) lines with reduced lignin contents, Bioenergy Res. 2 (2009) 153–164, http://dx.doi.org/10.1007/s12155-009-9041-2.
[16] S.E. Sattler, D.L. Funnell-Harris, J.F. Pedersen, Brown midrib mutations and their importance to the utilization of maize, sorghum, and pearl millet lignocellulosic tissues, Plant Sci. 178 (2010) 229–238, http://dx.doi.org/10.1016/j.plantsci.2010.01.001.
[17] C.E. Shoemaker, D.I. Bransby, The role of sorghum as a bioenergy feedstock in sustainable alternative fuel feedstock opportunities, challenges and roadmaps for six US regions, in: Sustainable Feedstocks for Advanced Biofuels Workshop; 28-30 September 2010; Atlanta, USA. Proceedings, 2010, pp. 28–30.
[18] M. Claussen, V. Brovkin, A. Ganopolski, Biogeophysical versus biogeochemical feedbacks of largerscale land cover change, Geophys. Res. Lett. 28 (2001) 1011–1014, http://dx.doi.org/10.1029/2000GL012471.
[19] J.H. Rydsaa, F. Stordal, L.M. Tallaksen, Sensitivity of the regional European boreal climate to changes in surface properties resulting from structural vegetation perturbations, Biogeosciences 12 (2015) 3071–3087, http://dx.doi.org/10.5194/bg-12-3071-2015.
[20] D.D. Baldocchi, Assessing the eddy covariance technique for evaluating carbon dioxide exchange rates of ecosystems: past, present and future, Glob. Chang. Biol. 9 (2003) 479–492, http://dx.doi.org/10.1046/j.1365-2486.2003.00629.x.
[21] R.G. Anderson, D. Wang, Energy budget closure observed in paired Eddy Covariance towers with increased and continuous daily turbulence, Agric. For. Meteorol. 184 (2014) 204–209, http://dx.doi.org/10.1016/j.agrformet.2013.09.012.
[22] N. Rajan, S. Maas, S. Cui, Extreme drought effects on evapotranspiration and energy balance of a pasture in the Southern Great High Plains, Ecohydrology (2015) 1194–1204, http://dx.doi.org/10.1002/eco.1574.
[23] B. Law, Ameriflux network aids global synthesis, Eos. Trans. Amer. Geophys. Union 88 (2007) 286–297.
[24] P. Wagle, V.G. Kakani, R.L. Huhnke, Evapotranspiration and ecosystem water use efficiency of switchgrass and high biomass sorghum, Agron. J. 108 (2016) 1007–1019, http://dx.doi.org/10.2134/agronj2015.0149.
[25] N. Rajan, S.J. Maas, Spectral crop coefficient approach for estimating daily crop water use, Adv. Remote Sens. 03 (2014) 197–207, http://dx.doi.org/10.4236/ars.2014.33013.
[26] J.B. Moncrieff, J.M. Massheder, H. de Bruin, J. Elbers, T. Friborg, B. Heusinkveld, P. Kabat, S. Scott, H. Soegaard, A. Verhoef, A system to measure surface fluxes of momentum, sensible heat, water vapour and carbon dioxide, J. Hydrol 188–189 (1997) 589–611, http://dx.doi.org/10.1016/S0022-1694(96)03194-0.
[27] R. Webb, E.K. Pearman, G.I. Leuning, Correction of flux measurements for density effects due to heat and water vapour transfer, Q. J. R. Meteorol. Soc. 106 (1980) 85–100, http://dx.doi.org/10.1002/qj.49710644707.
[28] T. Foken, M. Gockede, M. Mauder, L. Mahrt, B.D. Amiro, J.W. Munger, Post field data quality control, in: X. Lee, W. Massman, B. Law (Eds.), Hand-book of Micrometeorology, Springer, 2004, p. 181.
[29] M. Göckede, T. Foken, M. Aubinet, M. Aurela, J. Banza, C. Bernhofer, J.M. Bonnefond, Y. Brunet, A. Carrara, R. Clement, Quality control of CarboEurope flux data–Part I: footprint analyses to evaluate sites in forest ecosystems, Biogeosci. Discuss. 4 (2007) 4025–4066, http://dx.doi.org/10.5194/bg-5-433-2008.
[30] N. Rajan, S. Maas, S. Cui, Extreme drought effects on carbon dynamics of a semi-arid pasture, Agron. J. (2013) 1749–1760.
[31] E. Falge, D.D. Baldocchi, R. Olson, P. Anthoni, M. Aubinet, Gap filling stratergies for defansible annual sums of net ecosystem exchange, Agric. For. Meteorol 107 (2001) 43–69.
[32] M. Reichstein, D. Papale, R. Valentini, M. Aubinet, C. Bernhofer, A. Knohl, T. Laurila, A. Lindroth, E. Moors, K. Pilegaard, G. Seufert, Determinants of terrestrial ecosystem carbon balance inferred from European eddy covariance flux sites, Geophys. Res. Lett. 34 (2007) 1–5, http://dx.doi.org/10.1029/2006GL027880.
[33] J. Lloyd, J.A. Taylor, On the temperature dependence of soil repiration, Funct. Ecol. 8 (1994) 315–323.
[34] T. Foken, The energy balance closure problem: an overview, Ecol. Appl. 18 (2008) 1351–1367.
[35] N. Rajan, S.J. Maas, J.C. Kathilankal, Estimating crop water use of cotton in the Texas High Plains, Agron. J. 102 (4) (2010) 1641–1651.
[36] J.L. Steiner, Dryland grain sroghum water use, light interception, and growth responses to planting geometry, Agron. J. 78 (1986) 720–726.
[37] G.W. Wall, E.T. Kanemasu, Carbon dioxide exchange rates in wheat canopies. Part I. Influences of canopy geometry on trends in leaf area index, light interception and instantaneous exchange rates, Agric. For. Meteorol 49 (1990) 81–102.
[38] A. Kross, H. McNairn, D. Lapen, M. Sunohara, C. Champagne, Assessment of RapidEye vegetation indices for estimation of leaf area index and biomass in corn and soybean crops, Int. J. Appl. Earth Obs. Geoinf 34 (2015) 235–248, http://dx.doi.org/10.1016/j.jag.2014.08.002.
[39] Y. Song, A.K. Jain, W. Landuyt, H.S. Kheshgi, M. Khanna, Estimates of biomass yield for perennial bioenergy grasses in the USA, Bioenergy Res. 8 (2015) 688–715, http://dx.doi.org/10.1007/s12155-014-9546-1.
[40] P.Y. Oikawa, G.D. Jenerette, D.A. Grantz, Offsetting high water demands with

high productivity: sorghum as a biofuel crop in a high irradiance arid ecosystem, GCB Bioenergy 7 (2015) 974–983, http://dx.doi.org/10.1111/gcbb.12190.
[41] M.P. Singh, J.E. Erickson, L.E. Sollenberger, K.R. Woodard, J.M.B. Vendramini, J.R. Fedenko, Mineral composition and biomass partitioning of sweet sorghum grown for bioenergy in the southeastern USA, Biomass Bioenergy 47 (2012) 1–8, http://dx.doi.org/10.1016/j.biombioe.2012.10.022.
[42] J. Cotton, G. Burow, V. Acosta-Martinez, J. Moore-Kucera, Biomass and cellulosic ethanol production of forage sorghum under limited water conditions, Bioenergy Res. 6 (2013) 711–718, http://dx.doi.org/10.1007/s12155-012-9285-0.
[43] M.E. McCormik, M.E. Morris, B.A. Ackerson, D.C. Blouin, Ratoon cropping forage sorghum for silage: yieldm fermentation, and Nutrition, Agron. J. 87 (1995) 952–957, http://dx.doi.org/10.2134/agronj1995.00021962008700050030x.
[44] S. Livingston, C.G. Coffmanm, Ratooning Grain Sorghum on the Texas Gulf Coast, Agrilife Extension, Texas A&M University, 1997.
[45] B. Venuto, B. Kindiger, Forage and biomass feedstock production from hybrid forage sorghum and sorghum-ssudangrass hybrids, Grassl. Sci. 54 (2008) 189–196, http://dx.doi.org/10.1111/j.1744-697X.2008.00123.x.
[46] J.L. Montieth, Climate and the efficiency of crop production in Britain, Philos. T. Roy. Soc. B 281 (1977) 277–294.
[47] J.M. Chen, T.A. Black, Defining leaf area index for non-flat leaves, Plant. Cell Environ. 15 (1992) 421–429, http://dx.doi.org/10.1111/j.1365-3040.1992.tb00992.x.
[48] R.L. Scott, J.A. Biederman, Partitioning evapotranspiration using long-term carbon dioxide and water vapor fluxes, Geophys. Res. Lett. (2017) 1–8, http://dx.doi.org/10.1002/2017GL074324.
[49] A. Hammerle, A. Haslwanter, U. Tappeiner, A. Cernusca, G. Wohlfahrt, Leaf area controls on energy partitioning of a mountain grassland, Biogeosci. Discuss. 4 (2007) 3607–3638, http://dx.doi.org/10.5194/bgd-4-3607-2007.
[50] P.B. Alton, P.R. North, S.O. Los, The impact of diffuse sunlight on canopy light-use efficiency, gross photosynthetic product and net ecosystem exchange in three forest biomes, Glob. Change Biol. 13 (4) (2007) 776–787.
[51] J.W. Jans, C.M. Jacobs, B. Kruijt, J.A. Elbers, S. Barendse, E.J. Moors, Carbon exchange of a maize (Zea mays L.) crop: influence of phenology, Agric. Ecosys. Environ. 139 (3) (2010) 316–324.
[52] P. Wagle, V.G. Kakani, R.L. Huhnke, Evapotranspiration and ecosystem water use efficiency of switchgrass and high biomass sorghum, Agron. J. 108 (2016) 1007–1019, http://dx.doi.org/10.2134/agronj2015.0149.
[53] M.P. Bange, G.L. Hammer, K.G. Rickert, Effect of specific leaf nitrogen on radiation use efficiency and growth of sunflower, Crop Sci. 37 (1997) 1201–1207.
[54] Y. Nouvellon, A. Bégué, M. Susan Moran, D. Lo Seen, S. Rambal, D. Luquet, G. Chehbouni, Y. Inoue, PAR extinction in shortgrass ecosystems: effects of clumping, sky conditions and soil albedo, Agric. For. Meteorol 105 (2000) 21–41, http://dx.doi.org/10.1016/S0168-1923(00)00194-5.
[55] N.J.J. Bréda, Ground-based measurements of leaf area index: a review of methods, instruments and current controversies, J. Exp. Bot. 54 (2003) 2403–2417, http://dx.doi.org/10.1093/jxb/erg263.
[56] P.L. Nagler, E.P. Glenn, T. Lewis Thompson, A. Huete, Leaf area index and normalized difference vegetation index as predictors of canopy characteristics and light interception by riparian species on the Lower Colorado River, Agric. For. Meteorol 125 (2004) 1–17, http://dx.doi.org/10.1016/j.agrformet.2004.03.008.
[57] T. Ise, C.M. Litton, C.P. Giardina, A. Ito, Comparison of modeling approaches for carbon partitioning: impact on estimates of global net primary production and equilibrium biomass of woody vegetation from MODIS GPP, J. Geophys. Res. Biogeosci. 115 (2010) 1–11, http://dx.doi.org/10.1029/2010JG001326.
[58] M. Campioli, S. Vicca, S. Luyssaert, J. Bilcke, E. Ceschia, F.S. Chapin III, P. Ciais, M. Fernández-Martínez, Y. Malhi, M. Obersteiner, D. Olefeldt, D. Papale, S.L. Piao, J. Peñuelas, P.F. Sullivan, X. Wang, T. Zenone, I.A. Janssens, Biomass production efficiency controlled by management in temperate and boreal ecosystems, Nat. Geosci. 8 (2015) 843–846, http://dx.doi.org/10.1038/ngeo2553.
[59] I.R. Johnson, J.H.M. Thornley, A model of shoot:root partioning with optimal growth, Ann. Bot. 60 (1987) 133–142.
[60] A. Blum, G.F. Arkin, Sorghum root growth and water-use as affected by water supply and growth duration, Field Crops Res. 9 (1984) 131–142.
[61] P. Barbieri, L. Echarte, A. della Maggiora, V.O. Sadras, H. Echeverria, F.H. Andrade, Maize evapotranspiration and water-use efficiency in response to row spacing, Agron. J. 104 (2012) 939–944, http://dx.doi.org/10.2134/agronj2012.0014.
[62] E. Eichelmann, C. Wagner-Riddle, J. Warland, B. Deen, P. Voroney, Carbon dioxide exchange dynamics over a mature switchgrass stand, GCB Bioenergy 8 (2016) 428–442, http://dx.doi.org/10.1111/gcbb.12259.
[63] M. Abraha, I. Gelfand, S.K. Hamilton, C. Shao, Y.J. Su, G.P. Robertson, J. Chen, Ecosystem water-use efficiency of annual corn and perennial grasslands: contributions from land-use history and species composition, Ecosystems 19 (2016) 1001–1012, http://dx.doi.org/10.1007/s10021-016-9981-2.